

COMBUSTION MODELLING IN A TWO-STROKE COPPER COATED SPARK IGNITION ENGINE

ABSTRACT

Investigations were carried out to evaluate the combustion parameters experimentally for a two-stroke copper coated (copper of thickness 300 microns was coated on the piston crown and cylinder head) spark ignition engine of brake power 2.2 kW at a speed of 3000 rpm, and were correlated with two-zone and multi-zone combustion models. Multi-zone combustion model gave results very close (deviation being 7%) to experimental values, while two-zone combustion model deviated from actual (experimental) results by 9%.

KEYWORDS: S.I. Engine, Two zone combustion model, CE, CCE, Combustion characteristics.

1. INTRODUCTION

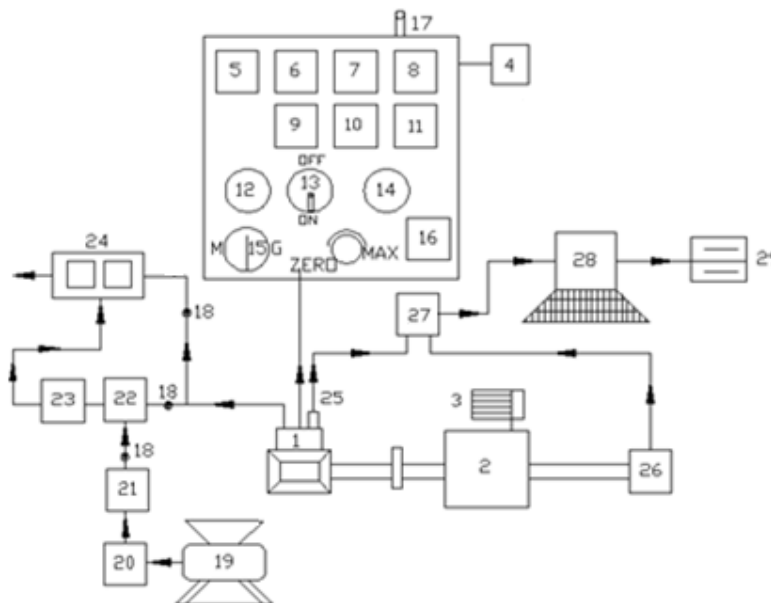
Petrol engines are superior to diesel engines as they produce less vibration and provide more comfort. Two stroke engines develop more power when compared with four stroke engines. There are many methods to improve the performance of the engine out of which copper coating on engine components is one of the simple techniques. Murali Krishna *et al.* [1,2] and Murthy *et al.* [3] presented the performance of four-stroke, single cylinder SI engine with alcohol (20% alcohol, 80% gasoline, by vol) having CCE provided with catalytic converter with manganese ore/sponge iron as catalyst and compared with conventional SI engine with gasoline operation. Brake thermal efficiency increased with gasohol with both versions of the engine. CCE showed improved performance when compared to CE with both test fuels. There are many combustion models developed for gasoline engines and out of which some models are presented below. A comprehensive simulation model for a spark ignition engine including intake and exhaust systems was presented (Benson *et al.* [4] and Gatowski *et al.* [5]) The predicted NO results were compared with test results found that good agreement between the predicted and measured NO over an equivalence range of 0.8-1.1 when the flame speed is corrected at the equivalence (0.9) corresponding to the peak NO was obtained. Paulina [6] attempts to accurately predict the gas pressure changes within the cylinder of a spark-ignition engine using thermodynamic principles. The model takes into account the intake, compression, combustion, expansion and exhaust processes that occur in the cylinder. Comparisons with actual pressure data show the model to have a high degree of accuracy. The model is further evaluated on its ability to predict the angle of spark firing and burn duration. Ivan Arsie *et al.* [7] predicted main thermodynamic model, which was based on classical two-zone approach for the simulation of performance and emissions in an SI engine. A multi-zone model was derived from two-zone calculations for a proper evaluation of temperature gradient in the burned gas region. The emissions of HC, CO and NO_x were predicted by three sub-models. Van Leersum *et al.* [8] studied the numerical model of the main processes occurring in a two-stroke internal combustion engine are described. Numerical, convergence, and flux conservation properties of the model are illustrated and engine performances predicted by it are shown to compare well with experimental data from a high performance 125cc engine and a medium performance 100 cc engine. Chan *et al.* [9] developed modeling of an engine in cylinder thermodynamics under high values of ignition retard, with the objective of improving exhaust gas availability for heating so that rapid catalyst light off can be achieved at engine cold-start. Modified Wiebe function was used in conjunction with an empirical correlation for cylinder pressure variation during the mass blow down process, which occurs between the exhaust valves opened and bottom dead centre (BDC). Nedunchezian *et al.* [10] formulated a heat release analysis procedure for a two-stroke SI engine. The model was used to

calculate instantaneous heat release rates, cumulative heat release and mass fraction burned off base engine and catalytic engine. The combustion chamber of the catalytic engine was coated with a catalyst material by plasma spraying method. The tests were conducted with different air-fuel ratios and heat release analysis was carried out for both CE and CCE. The average of these traces was calculated and is used as input to the heat release model. From the heat release rate, various combustion characteristics, such as delay period, start of combustion, end of combustion and combustion duration were calculated for the CE and CCE. The results indicate that the heat release model could be used for the calculation of combustion parameters and accurate enough for the present purpose. Sithiracha *et al.* [11] developed a mathematical model for an SI engine using cylinder-by-cylinder model approach in order to predict the performances, torque and power. The developed model consists of a set of tuning parameters such as engine physical geometries, ignition advance, air/fuel ratio, etc.. Harish Kumar *et al.* [12] developed a 'logistic model with conditional variability for precise simulation of combustion in SI engines as the model has built in routines to take into account such factors as location of spark plug, single/dual spark plugs, intake generated swirl, combustion chamber geometry (associated with Bore/Stroke ratio), etc. Nirendra *et al.* [13] emphasized that, engine simulation tools play an important role in such investigations without performing the experimental works An extended investigation is done for the NO_x emissions considering multiple burn zones. The results are verified against those obtained experimentally for engine torque/brake power, exhaust temperature, and exhaust emissions. A good agreement was found between them. Hosseini *et al.* [14] developed a model which concern to the combustion of a four-stroke, single cylinder, Ricardo E6 research engine. Work has been carried out in development of a comprehensive program aimed at accurately simulating SI engine combustion over a wide range of operating conditions. The accuracy determinations are considered with regard to speed, spark timing, compression ratio, and equivalence ratio in cylinder pressure versus crank angle diagrams. After model adjustment for matching the simulated pressure data with experimental data, it was found that heat transfer model of Annand was found to have better influence on matching experimental data. Verhelst *et al.* [15] proposed a unified framework that could be used to compare different sub-models on the same basis, with particular focus on turbulent combustion models. They reported that multi-zone thermodynamic models could provide a valuable tool for understanding and development of combustion in SI engines. They sub-modeled multi-zone engine modeling as blow-by, heat transfer, burned gas composition, mass burning rate and $\kappa - \epsilon$ type models { Agarwal *et al.* [16] }. The mass burning rate model was further classified in to different phases: ignition modeling in which set-off equations were given, initial phase of combustion, fully developed turbulent combustion, end of combustion and laminar burning velocity. They also included modeling of emissions and abnormal combustion phenomena. While doing so, depending on the method of initialization, the calculation of mass burning rate and a part of the flame development phase was effectively skipped. They gave basic equations for the engine model, derived from the conservation of energy applied to cylinder volume. Vancoillie et al. [17] studied the use of methanol and ethanol in internal combustion engines forms an interesting approach to decarburizing transport and securing domestic energy supply. This paper discusses the requirements for the construction of a two-zone thermodynamic model that can predict the power cycle, pollutant emissions and knock onset in alcohol engines. Aleonte et al. [18] conducted experiment on direct injection spark ignition engines in order to optimize the combustion process. This paper presents two methods, which were used to improve the combustion process and its exhaust emission in a two stroke SI engine. Comparisons are made with other engine fuelling systems, regarding the combustion process and the resulting emissions. Farag *et al.* [19] studied the quasi dimensional spark ignition engine cycle model to predict the cycle performance and exhaust emissions of an engine for the cases of using gasoline, CNG and hydrogen. The model consists of two different thermodynamic regions consisting of unburned gases and burned gases that are separated by the flame front. Governing

equations of the mathematical model mainly consist of first order differential equations derived for cylinder pressure and temperature. A computer code for the cycle model has been prepared to perform numerical calculations over a range of fuel-air equivalence ratios. Comparisons show that if spark ignition engine fuelled with hydrogen and CNG, there would be a reduction in exhaust emissions and enhancements in performance parameters more than that of gasoline fuel. Jiri Hvezda *et al.* [20] focused on simulation of high-pressure part of thermodynamic cycle in a four-stroke spark ignition engine. The main author's ambition is to create the fast and sufficiently accurate multi-zone simulating tool working on the basis of simple quasi-dimensional method reflecting a real 3-D combustion chamber geometry and using the specific approach to transfer and transformation of species. The introduced procedure combines a classical kinetic scheme with the flexible Holub's method for chemical equilibrium to solve serious numerical issues resulting from chemical kinetics itself. Lounici *et al.* [21] presented a two-zone model which is one of the most interesting engine simulation tools, especially for SI engines. The current study aims to investigate the effect of the choice of both the heat transfer correlation and burned zone heat transfer area calculation method and provide an optimized choice for a more efficient two-zone thermodynamic model, in the case of natural gas SI engines. For this purpose, a computer simulation is developed. Experimental measurements are carried out for comparison and validation. The effect of correlation choice has been first studied. It is found that Hohenberg's correlation is the best choice. However, the influence of the burned zone heat transfer area calculation method is negligible.

2. MATERIALS AND METHODS

The two-stroke, single-cylinder, air-cooled, Bajaj make, petrol engine (square engine) of brake power 2.2 kW at 3000 rpm with a compression ratio of 7.5:1 is used in the experimentation. The test fuels used for experimentation are pure gasoline and methanol blended gasoline (20% of methanol blended with 80% of gasoline, by volume). The schematic diagram of experimental set up employed to evaluate the performance parameters is shown in Fig-1.



1.Engine, 2.Electrical swinging field dynamometer, 3. Loading arrangement, 4.Fuel tank, 5.Torque indicator/controller sensor, 6. Fuel rate indicator sensor, 7. Hot wire gas flow indicator, 8. Multi channel temperature indicator, 9. Speed indicator, 10. Air flow indicator,11. Exhaust gas temperature indicator, 12.

Mains ON, 13. Engine ON/OFF switch, 14. Mains OFF, 15. Motor/Generator option switch, 16. Heater controller, 17. Speed indicator, 18. Directional valve, 19. Air compressor, 20. Rotometer, 21. Heater, 22. Air chamber, 23. Catalytic chamber, 24. CO/HC analyzer, 25. Piezoelectric transducer, 26. TDC encoder, 27. Consol, 28. Pentium personal computer, 29. Printer.

Figure 1 Schematic diagram of the experimental set up

The fuel consumption, speed, torque, air flow rate and exhaust gas temperature are indicated with electronic sensors. The engine oil is provided with a pressure-feed system. Piezo electric transducer, fitted on the cylinder head to measure the pressure in the combustion chamber is connected to a console, which in turn is connected to a Pentium personal computer. TDC encoder provided at the extended shaft of the dynamometer is connected to the console to measure the crank angle of the engine. A special P- θ software package evaluates the combustion characteristics such as peak pressure (PP), time of occurrence of peak pressure (TOPP), maximum rate of pressure rise (MRPR) and maximum heat release (MHR) from the signals of P- θ software at peak load operation of the engine. Pressure-crank angle diagram and heat release-crank angle diagram were obtained on the screen of the personal computer.

3. COMBUSTION MODELING

Computer simulation is the process of formulating a model of a physical system representing the actual processes and analyzing the same. Usually the model is a mathematical one representing the actual processes through a set of algebraic differential or integral equations and the analysis is made using a computer.

In an Internal combustion engine, the processes involved are extremely complex. Computer simulation offers the advantages like it serves as a tool for better understanding of the variables involved and their effect on the engine performance. It systematizes the knowledge obtained through expensive testing. It considerably reduces the time consuming tests by narrowing down the variables that must be studied and it helps in optimizing the engine design for a particular application, reducing cost and time.

3.1 Description of two-zone combustion model

The combustion chamber is divided into two zones, corresponding to burned and unburned gas regions, by an infinitesimal flame front with a spherical shape. In each zone the thermodynamic state is defined by the mean thermodynamic properties; the burned gas are assumed in chemical equilibrium during combustion and for the main expansion stroke, while near the end of the expansion process the mixture is assumed frozen [7].

3.1.1 Assumptions

To analyze and reduce the complexity of the problem, certain assumptions are made while modeling the combustion process in a copper coated SI engine.

(i) Conservation of fuel-air mixture (ii) Mixing is complete, (iii) Pressure and volume remain constant, (iv) Conservation of energy, (v) Crevice losses may be significant but are not included, and (vi) constant specific heats

The two-zone combustion modelling is carried out with constant specific heats and with variable specific heats, which was explained in the following sections.

3.1.2 Two-zone combustion model

The conditions in the burned and unburned gas are determined [22] by conservation of mass:

$$\frac{V}{m} = \int_0^{x_b} v_b dx + \int_{x_b}^1 v_u dx \quad (1)$$

where, $V = V_u + V_b$

$$x_b = \frac{m_b}{m}$$

and, $m = m_u + m_b$

by conservation of energy, one can get:

$$\frac{U_0 - W - Q}{m} = \int_0^{x_b} u_b dx + \int_{x_b}^1 u_u dx \quad (2)$$

From the ideal gas law, x_b can be found out by the relation [22]:

$$x_b = \left[1 + \frac{\rho_u}{\rho_b} \left(\frac{1}{y_b} - 1 \right) \right]^{-1} \quad (3)$$

where, $y_b = \frac{v_b}{v}$

While the density ratio $\left(\frac{\rho_u}{\rho_b} \right)$ does not depend on the equivalence ratio, burned gas fraction in the unburned mixture, and pressure, its value is close to 4 for most SI engine operating conditions.

A functional form often used to represent the mass fraction burned versus crank angle curve is the Wiebe function [23]:

$$x_b = 1 - \exp \left[-a_1 \left(\frac{\theta - \theta_0}{\Delta\theta} \right)^{a_2} \right] \quad (4)$$

Varying a_1 and a_2 changes the shape of the curve significantly. Actual mass fraction burned curves have been fitted with $a_1 = 5$ and $a_2 = 3$.

The work and heat transfers are given by the relation [22]:

$$W = \int_{v_0}^v p dV' \quad (5)$$

$$Q = \int_{\theta_0}^{\theta} \left(\frac{\dot{Q}}{360N} \right) d\theta \quad (6)$$

Where, \dot{Q} can be calculated from the relation [22],

$$\dot{Q} = \frac{dQ}{dt} = A h_c (T - T_w) \quad (7)$$

The heat transfer between gas and cylinder walls is given by [7]:

$$\frac{dQ}{d\theta} = \frac{-\dot{Q}_l}{\omega} = \frac{-\dot{Q}_b - \dot{Q}_u}{\omega} \quad (8)$$

The two heat flux terms for burned and unburned gases are modeled [7] as follows:

$$\dot{Q}_b = h_{c,b} A_b (T_b - T_w) \quad (9)$$

$$\dot{Q}_u = h_{c,u} A_u (T_u - T_w) \quad (10)$$

The surface areas A_b and A_u are computed as function of D and V with the following relations [7]:

$$A_b = \left(\frac{\pi D^2}{2} + \frac{4V}{D} \right) X_b^{\frac{1}{2}} \quad (11)$$

$$A_u = \left(\frac{\pi D^2}{2} + \frac{4V}{D} \right) (1 - X_b)^{\frac{1}{2}} \quad (12)$$

It is assumed that the burned gas contact wall surface is proportional to the square root of burned mass fraction to account for the greater volume filled by burned gases with respect to unburned ones.

Now, h_c is computed from the well known correlation proposed by Woschni [24] as function of

D , p , T and w as:

$$h_c = 326 D^{-0.2} p^{0.8} T^{-0.55} w^{0.8} \quad (13)$$

In the equation-13, w is related to the mean piston speed \bar{S}_p and combustion phenomena [25, 22]:

$$w = \left[C_1 \bar{S}_p + C_2 \frac{v_{Tf}}{F_T V_T} (p - p_m) \right] \quad (14)$$

The constants C_1 and C_2 are derived from Woschni [24].

Accurate calculations of the state of the cylinder gases require an equilibrium model (or good approximation to it) for the burned gas and an ideal gas mixture model (of frozen composition) for the unburned gas. However, useful results can be obtained by assuming that the burned and unburned gases are different ideal gases, each with constant specific heats [26];

$$\text{i.e., } p v_b = R_b T_b \quad u_b = c_{v,b} T_b + h_{f,b} \quad (15)$$

$$p v_u = R_u T_u \quad u_u = c_{v,u} T_u + h_{f,u} \quad (16)$$

Combining equations 1, 2, 5, 6, 15 and 16,

$$\frac{pV}{m} = x_b R_b \bar{T}_b + (1 - x_b) R_u \bar{T}_u \quad (17)$$

$$\text{and, } \frac{U_o - W - Q}{m} = x_b (c_{v,b} \bar{T}_b + h_{f,b}) + (1 - x_b) (c_{v,u} \bar{T}_u + h_{f,u}) \quad (18)$$



$$\text{where, } \bar{T}_b = \frac{1}{x_b} \int_0^{x_b} T_b dx \quad (19)$$

$$\text{and, } \bar{T}_u = \frac{1}{1-x_b} \int_{x_b}^1 T_u dx \quad (20)$$

Equations 17 and 18 may now be solved to obtain

$$X_b = \frac{p V - p_0 V_0 + (\gamma_b - 1)(W + Q) + (\gamma_b - \gamma_u) m c_{v,u} (\bar{T}_u - T_0)}{m [(\gamma_b - 1)(h_{f,u} - h_{f,b}) + (\gamma_b - \gamma_u) c_{p,u} \bar{T}_u]} \quad (21)$$

$$\text{and, } \bar{T}_b = \frac{R_u}{R_b} \bar{T}_u + \frac{pV - mR_u \bar{T}_u}{mR_b X_b} \quad (22)$$

If it is now assumed that the burned gas is initially uniform and undergoes isentropic compression, then [22]:

$$\frac{\bar{T}_u}{T_0} = \left(\frac{p}{p_0} \right)^{(\gamma_u - 1)/\gamma_u} \quad (23)$$

This equation 23 with equations 21 and 22 enables determination of both X_b and \bar{T}_b , from the thermodynamic properties of the burned and unburned gases, and known values of p , V , m , and Q . Alternatively, if X_b is known then p can be determined. Mass fraction burned and cylinder gas pressures are uniquely related.

Neglecting the volume occupied by the fuel in the crevices, the heat release rate can be found out using the following relation [22]:

$$\frac{dQ_{GR}}{d\theta} = \left(\frac{\gamma}{\gamma - 1} \right) p \frac{dV}{d\theta} + \left(\frac{1}{\gamma - 1} \right) V \frac{dp}{d\theta} \quad (24)$$

3.1.3 Solution procedure

Equations 1, 2, 4, 5, 6, 7, 8, 9, 10, 17, 18, 19, 20, 21, 22 and 24 formed the set of governing equations for gasoline operation as well as for methanol blended gasoline operation, which are solved using Runge-Kutta 4th order scheme. Computerization started at EPO and closed at EPC.

3.2 Description of multi-zone combustion model

To account for different gas composition and temperature gradients occurring in the various combustion chamber regions (e.g. spark plug, piston head), the burned gas volume is divided into N^* zones representing an adiabatic core region. A further external zone has been also considered as thermal boundary region of the central adiabatic core zones, primarily responsible for the heat transfer. It is assumed that no mixing occurs between neighboring zones and that at the end of combustion the same mass fraction is present in each zone. This schematization is consistent with the hypothesis that burned gases experience a continuous adiabatic compression process as the combustion proceeds [22, 28].

The basis for multi-zone models is formed by consideration of conservation of mass and energy. In the following sections, the equations for the cylinder pressure and temperature(s) are derived.

3.2.1 Assumptions

Before conservation of energy is written out for the cylinder volume, from inlet valve closing time to exhaust valve opening time (i.e. the power cycle), some assumptions are generally adopted to simplify the equations. i) During compression and expansion, pressure is invariably assumed uniform throughout the cylinder, with fixed unburned and burned gas regions in chemical equilibrium. and (ii) During flame propagation, burned and unburned zones are assumed to be separated by an infinitely thin flame front, with no heat exchange between the two zones.

3.2.2 Sub-zones in multi-zone combustion model

In summary, multi-zone engine modeling requires sub-models for:

- i) Blow-by, ii) Heat transfer, iii) Burned gas composition, iv) Mass burning rate
- In-cylinder turbulence, as needed by the heat transfer and mass burning rate sub-models either based on experimentally derived data, or from cold flow CFD calculations [15].

The basic equation for the engine model is derived from the conservation of energy applied to the cylinder volume [15]:

$$dU = -\delta Q - \delta W + \sum_i h_i dm_i \quad (25)$$

In the equation-25, $Q > 0$ for heat loss from gas to wall and $W > 0$ for work delivered by the cylinder charge. The work can be calculated by the relation [22]: $\delta W = p dV$

The first term on the right hand side of Eq. (25) expresses the heat loss of the cylinder contents to the surroundings. The second term expresses the work delivered; the third term is the total energy flowing into or out of the cylinder. Here, only the power cycle is considered so the change in cylinder mass is solely through blow-by.

In the following sections Eq. (25) is developed for the cases compression/expansion and combustion. Here, this is done on a mass basis but the equations can also be cast in molar form.

3.2.3 Heat transfer model

Heat transfer to cylinder walls is obtained by using Annand's relation [29]. This relation considers the net heat transfer as the summation of both convective and radiative heat transfer.

$$\frac{dQ_w}{dt} = \frac{aAK}{D} [(Re)^b] [T - T_w] + A c (T^4 - T_w^4) \quad (26)$$

In the equation-26, the value of the factor 'a' varies widely with intensity of the charge motion. With normal combustion, the value should be selected in between 0.35 and 0.8 and it increases with the intensity of the motion in the region being considered. The term 'b' is the relative index of Nu to Re. The value of 'b' can be taken as 0.7 while, 'c' is the radiant heat constant. Possible values of 'c' appear to be, during compression, $c = 0$. During combustion and expansion,

$c = 1.6 \times 10^{-12}$ for petrol engines, and, $A = A_p + A_{hi} + A_h$

The wall temperature is obtained based on FEM analysis carried out for copper coated engine.

3.2.4 Multi-zone model during compression and expansion

Starting from conservation of energy, with the change in cylinder mass solely from blow-by, following equation [15] can be obtained:

$$\frac{d(mu)}{d\theta} = - \frac{dQ}{d\theta} - p \frac{dV}{d\theta} + h \frac{dm}{d\theta} \quad (27)$$

The left hand side of Eq. (27) i.e., $\left[\frac{d(mu)}{d\theta} \right]$ can be written as [15]:

$$\frac{d(mu)}{d\theta} = m \frac{du}{d\theta} + u \frac{dm}{d\theta} \quad (28)$$

with $\frac{du}{d\theta} = \frac{\partial u}{\partial T} \cdot \frac{dT}{d\theta} = C_v \frac{dT}{d\theta}$.

and $\frac{dm}{d\theta}$ resulting from blow-by: $\frac{dm}{d\theta} = \frac{dm_1}{d\theta}$.

3.2.5 Temperature change

For an ideal gas, $h = u + R T$, resulting in the following equation [15] for the temperature change:

$$\frac{dT}{d\theta} = \frac{1}{m c_v} \left[- \frac{dQ}{d\theta} - p \frac{dV}{d\theta} + \frac{dm}{d\theta} RT \right] \quad (29)$$

3.2.6 Pressure from conservation of momentum

For the pressure change, the ideal gas equation $pV = mRT$ is differentiated [15]:

$$V \frac{dp}{d\theta} + p \frac{dV}{d\theta} = R T \frac{dm}{d\theta} + m T \frac{dR}{d\theta} + m R \frac{dT}{d\theta} \quad (30)$$

During compression, the cylinder gas composition can be assumed constant, during expansion it can be assumed to change only slowly, or $\frac{dR}{d\theta} \approx 0$, resulting in the following equation for the pressure

change [15]:

$$\frac{dp}{d\theta} = \frac{1}{V} \left[\frac{dm_1}{d\theta} RT + m R \frac{dT}{d\theta} - p \frac{dV}{d\theta} \right] \quad (31)$$



3.2.7 Multi-zone model during combustion

Conservation of energy applied to the unburned gas zone results in the following equation [15]:

$$\frac{dm_u u_u}{d\theta} = - \frac{dQ_u}{d\theta} - p \frac{dV_u}{d\theta} - h_u \frac{dm_x}{d\theta} - h_u \frac{dm_{l,u}}{d\theta} \quad (32)$$

here, $\frac{dm_{l,u}}{d\theta} > 0$.

Again, the left hand side can be written as:

$$m_u \frac{du_u}{d\theta} + u_u \frac{dm_u}{d\theta} \quad (33)$$

With $\frac{du_u}{d\theta} = C_{v,u} \frac{dT_u}{d\theta}$, the rate of change in the unburned gas can be written as:

$$\frac{dm_u}{d\theta} = - \frac{dm_x}{d\theta} - \frac{dm_{l,u}}{d\theta} \quad (34)$$

Resulting in:

$$m_u C_{v,u} \frac{dT_u}{d\theta} - u_u \frac{dm_x}{d\theta} = - \frac{dQ_u}{d\theta} - p \frac{dV_u}{d\theta} - h_u \frac{dm_x}{d\theta} - R_u T_u \frac{dm_{l,u}}{d\theta} \quad (35)$$

Conservation of energy for the burned gas zone results in [15]:

$$\frac{dm_b u_b}{d\theta} = - \frac{dQ_b}{d\theta} - p \frac{dV_b}{d\theta} + h_u \frac{dm_x}{d\theta} - h_b \frac{dm_{l,b}}{d\theta} \quad (36)$$

$$\text{Again, } \frac{dm_b u_b}{d\theta} = m_b \frac{du_b}{d\theta} + u_b \frac{dm_b}{d\theta} \quad (37)$$

With $\frac{du_b}{d\theta} = C_{v,b} \frac{dT_b}{d\theta}$, the rate of change in the burned mass can be written as:

$$\frac{dm_b}{d\theta} = - \frac{dm_x}{d\theta} - \frac{dm_{l,b}}{d\theta} \quad (38)$$

Resulting in:

$$m_b C_{v,b} \frac{dT_b}{d\theta} + u_b \frac{dm_x}{d\theta} = - \frac{dQ_b}{d\theta} - p \frac{dV_b}{d\theta} + h_u \frac{dm_x}{d\theta} - R_b T_b \frac{dm_{l,b}}{d\theta} \quad (39)$$

Next the total internal energy balance is written out, as the sum of the balances (38) and (39):

$$\begin{aligned} & m_u C_{v,u} \frac{dT_u}{d\theta} + m_b C_{v,b} \frac{dT_b}{d\theta} + (u_b - u_u) \frac{dm_x}{d\theta} \\ & = - \frac{dQ}{d\theta} - p \frac{dV}{d\theta} - R_u T_u \frac{dm_{l,u}}{d\theta} - R_b T_b \frac{dm_{l,b}}{d\theta} \end{aligned} \quad (40)$$

Using

$$\frac{dV}{d\theta} = \frac{dV_u}{d\theta} + \frac{dV_b}{d\theta} \quad (41)$$



$$\frac{dQ}{d\theta} = \frac{dQ_u}{d\theta} + \frac{dQ_b}{d\theta} \quad (42)$$

Differentiating the ideal gas equation for the two zones leads to [15]:

$$p \frac{dV_u}{d\theta} + V_u \frac{dp}{d\theta} = R_u T_u \frac{dm_u}{d\theta} + m_u R_u \frac{dT_u}{d\theta} \quad (43)$$

$$p \frac{dV_b}{d\theta} + V_b \frac{dp}{d\theta} = R_b T_b \frac{dm_b}{d\theta} + m_b R_b \frac{dT_b}{d\theta} \quad (44)$$

If equation (44) is used to substitute $p \frac{dV_u}{d\theta}$ in equation (36), one obtains the following equations

[15]:

$$\begin{aligned} & m_u c_{v,u} \frac{dT_u}{d\theta} - h_u - R_u T_u \frac{dm_u}{d\theta} \\ & = - \frac{dQ_u}{d\theta} - V_u \frac{dp}{d\theta} - R_u T_u \frac{dm_u}{d\theta} - m_u R_u \frac{dT_u}{d\theta} - h_u \frac{dm_u}{d\theta} - R_u T_u \frac{dm_{l,u}}{d\theta} \end{aligned} \quad (45)$$

$$\text{while, } c_{v,u} + R_u = c_{p,u} \quad (46)$$

Using the Eq. (45) and Eq. (36), the following equation is obtained for the rate of change of the unburned gas temperature:

$$\frac{dT_u}{d\theta} = \frac{1}{m_u c_{p,u}} \left[V_u \frac{dp}{d\theta} - \frac{dQ_u}{d\theta} \right] \quad (47)$$

Now, substituting $\frac{dV_u}{d\theta}$ and $\frac{dV_b}{d\theta}$ in equation 41 using equations 43 and 44, gives [15],

$$\frac{dV}{d\theta} = \frac{R_u T_u}{p} \frac{dm_u}{d\theta} + \frac{m_u R_u}{p} \frac{dT_u}{d\theta} - \frac{V_u}{p} \frac{dp}{d\theta} + \frac{R_b T_b}{p} \frac{dm_b}{d\theta} + \frac{m_b R_b}{p} \frac{dT_b}{d\theta} - \frac{V_b}{p} \frac{dp}{d\theta} \quad (48)$$

Using the ideal gas equation and equations 34 and 38, equation 48 can be rewritten as [15]:

$$\frac{dV}{d\theta} = \left[\frac{V_b}{m_b} - \frac{V_u}{m_u} \right] \frac{dm_{gr}}{d\theta} - \frac{V_u}{m_u} \frac{dm_{l,u}}{d\theta} - \frac{V_b}{m_b} \frac{dm_{l,b}}{d\theta} + \frac{V_u}{T_u} \frac{dT_u}{d\theta} + \frac{V_b}{T_b} \frac{dT_b}{d\theta} - \frac{V}{p} \frac{dp}{d\theta} \quad (49)$$

Rearranging this equation to obtain an equation for the rate of change of the burned gas temperature [15]:

$$\frac{dT_b}{d\theta} = \frac{p}{m_b R_b} \left[\frac{dV}{d\theta} - \left(\frac{V_b}{m_b} - \frac{V_u}{m_u} \right) \frac{dm_{gr}}{d\theta} + \frac{V_u}{m_u} \frac{dm_{l,u}}{d\theta} + \frac{V_b}{m_b} \frac{dm_{l,b}}{d\theta} + \frac{V}{p} \frac{dp}{d\theta} - \frac{V_u}{T_u} \frac{dT_u}{d\theta} \right] \quad (50)$$

3.2.8 Heat release rate

Heat release rate can be found using the following relation [22]:

$$\frac{dQ_{ch}}{d\theta} = \frac{\gamma}{\gamma-1} p \frac{dV}{d\theta} + \frac{1}{\gamma-1} V \frac{dp}{d\theta} + V_{cr} \left[\frac{T'}{T_w} + \frac{T}{T_w(\gamma-1)} + \frac{1}{b_2 T_w} \ln \left(\frac{\gamma-1}{\gamma-1} \right) \right] \frac{dp}{d\theta} + \frac{dQ_{ht}}{d\theta} \quad (51)$$

In the equation (5.70), γ is modeled with a linear function of temperature [22] as: $\gamma [T] = a_3 + b_3 T$



3.2.9 Pressure from conservation of momentum

Finally, substituting equations 47 and 50 in the equation 40 results in [15]:

$$\begin{aligned} & \frac{m_u c_{v,u}}{m_u c_{p,u}} \left[V_u \frac{dp}{d\theta} - \frac{dQ_u}{d\theta} \right] \\ & + \frac{m_b c_{v,b}}{m_b R_b} \left\{ \begin{aligned} & \frac{dV}{d\theta} - \left(\frac{v_b}{m_b} - \frac{v_u}{m_u} \right) \frac{dm_x}{d\theta} + \frac{v_u}{m_u} \frac{dm_{l,u}}{d\theta} + \frac{v_b}{m_b} \frac{dm_{l,b}}{d\theta} \\ & + \frac{v}{p} \frac{dp}{d\theta} - \frac{v_u}{m_u T_u c_{p,u}} \left(V_u \frac{dp}{d\theta} - \frac{dQ_u}{d\theta} \right) \end{aligned} \right\} \\ & + (u_b - u_u) \frac{dm_x}{d\theta} \\ & = - \frac{dQ}{d\theta} - p \frac{dV}{d\theta} - R_u T_u \frac{dm_{l,u}}{d\theta} - R_b T_b \frac{dm_{l,b}}{d\theta} \end{aligned} \quad (52)$$

Rearranging this equation to obtain the rate of change of the cylinder pressure [15]:

$$\begin{aligned} \frac{dp}{d\theta} &= \left(\frac{c_{v,u}}{c_{p,u}} - \frac{c_{v,b}}{R_b} \frac{R_u}{c_{p,u}} V_u + \frac{c_{v,b}}{R_b} v \right)^{-1} \\ & \left\{ \begin{aligned} & - \left(1 + \frac{c_{v,b}}{R_b} \right) p \frac{dV}{d\theta} - C_{p,b} T_b \frac{dm_{l,b}}{d\theta} \\ & - \frac{R_u}{R_b} C_{p,b} T_u \frac{dm_{l,u}}{d\theta} - \frac{dQ}{d\theta} - \left[u_b - u_u - c_{v,b} \left(T_b - \frac{R_u}{R_b} T_u \right) \right] \frac{dm_x}{d\theta} \\ & + \left(\frac{c_{v,u}}{c_{p,u}} - \frac{c_{v,b}}{R_b} \frac{R_u}{c_{p,u}} \right) \frac{dQ_u}{d\theta} \end{aligned} \right\} \end{aligned} \quad (53)$$

3.2.10 Rate of change of gas constant

Rate of gas constant can be derived from [30]:

$$R = \bar{R} \sum \frac{Y_{NS}}{W_{NS}} \quad (54)$$

Here, W = Molecular weight

By differentiating the expression (54),

$$\frac{dR}{dT} = \bar{R} \sum \frac{1}{M} \frac{dY_{NS}}{dt} \quad (55)$$

$$\text{but, } Y_{NS} = \frac{M_{NS}}{M} \quad (56)$$

here, M = mass

Differentiating the above equation (56)

$$\frac{dY_{NS}}{dT} = \frac{\dot{M}_{NS}}{M} - \frac{1}{M^2} \dot{M} M_{NS} = \frac{\dot{M}_{NS}}{M} - \frac{1}{M} \dot{M} \frac{M_{NS}}{M}$$

$$= \frac{\dot{M}_{NS}}{M} - \frac{\dot{M}}{M} Y_{NS} \quad (57)$$

By substituting the equation (57) in equation (55), one gets (30),

$$\frac{dR}{dI} = \bar{R} \sum \frac{1}{W_{NS}} \left[\frac{\dot{M}_{NS}}{M} - \frac{Y_{NS} \dot{M}}{M} \right] \quad (58)$$

3.2.11 Specific enthalpy

Specific enthalpy and specific heats of a gas of species 'i' are computed using the relation [32]:

In the lower temperature range ($400 \leq T \leq 1600^0$ K), the specific enthalpy and specific heats are computed as [32]:

$$h(T) = AL + (BL \times T) + CL \ln T \quad (\text{k J/mol}) \quad (59)$$

$$c_p(T) = BL + \frac{CL}{T} \quad (\text{k J/k mol-K}) \quad (60)$$

In the higher temperature range ($1600 \leq T \leq 6000^0$ K), the specific enthalpy and specific heats are computed as [32]:

$$h(T) = AH + (BH \times T) + CH \ln T \quad (\text{k J/mol}) \quad (61)$$

$$c_p(T) = BH + \frac{CH}{T} \quad (\text{k J/k mol-K}) \quad (62)$$

These coefficients are shown [32] in the reference. In order to compute the total molal enthalpy $h_{i,T}$ at a specified temperature and pressure other than the standard state, the change in enthalpy between the reference state and the specified state is to be added to the enthalpy of the formation (32).

$$h_{i,T} = h_{f_0} + (h_T - h_{298}) \quad (63)$$

Where h_{f_0} is calculated as the difference in enthalpy h_T at the specified temperature and h_{298} . Standard literature [33] gives the ideal gas enthalpy of different species at different temperature. If the tabular data are not available to evaluate the term sensible enthalpy change, it can be calculated as,

$$h_T - h_{298} = \int_{T_0}^T c_p dT \quad (64)$$

For each species 'i' in its standard state at temperature T^0 K, the specific heat $c_{p,i}$ is approximated by [22]:

$$c_{p,i} = R [a_{i1} + a_{i2} T + a_{i3} T^2 + a_{i4} T^3 + a_{i5} T^4] \quad (65)$$

The standard state enthalpy of species h_i is then given by [22]:

$$h_i = R T \left[a_{i1} + \frac{a_{i2}}{2} T + \frac{a_{i3}}{3} T^2 + \frac{a_{i4}}{4} T^3 + \frac{a_{i5}}{5} T^4 \right] \quad (66)$$

Values of the coefficients a_{ij} for CO₂, H₂O, CO, H₂, N₂, OH, NO, O and H are given [33] for temperature range 300 to 1000 °K for unburned mixture calculations and 1000 to 5000 °K range for burned mixture property calculations in NASA programme.

Polynomial functions for various fuels (in the vapor phase) have been fitted to the functional form [22]:

$$c_{p,v} = A_{f1} + A_{f2} t + A_{f3} t^2 + A_{f4} t^3 + \frac{A_{f5}}{t^2} \quad (67)$$

$$h_v = A_{f1} t + A_{f2} \frac{t^2}{2} + A_{f3} \frac{t^3}{3} + A_{f4} \frac{t^4}{4} - \frac{A_{f5}}{t} + A_{f6} + A_{f8} \quad (68)$$

In the equations (5.93 and 5.94), $t = \frac{T}{1000}$, here T is in °K

A_{f6} is the constant for the datum of zero enthalpy for C, H₂, O₂ and N₂ at 298.15 °K. For a 0 °K datum, A_{f8} is added to A_{f6} . For pure hydrocarbon compounds, the coefficients A_{fi} were found by the fitting the above equations to data from Rossini et al. [34]. The values of relevant pure fuels are given [22] in the reference. The units of $c_{p,v}$ are cal/gmol K and for h_v are kcal/g mols.

By knowing pressure and temperature of particular element, its volume can be found by applying the equation of state to individual element,

$$V_{ij} = \frac{M_{ij} R_{ij} T_{ij}}{p} \quad (69)$$

After finding the volume of all elements including the air element, the volume constraint should be checked. The volume constraint (where the liquid volume is neglected) is given by,

$$\sum V_{ij} = V_{\text{cycle}} \quad (70)$$

3.2.12 Rate of change of volume of charge

The rate of the charge in the cylinder at any crank angle can be calculated using the following [32] equations.

$$V_{dts} = V_{bds} - V_{tdc} = \frac{\pi}{4} D^2 S_c \quad (71)$$

$$V(\theta) = V_{dts} \left\{ \left(\frac{r_c}{r_c - 1} \right) - \left(\frac{1 - \cos \theta}{2} \right) + \left(\frac{L_c}{S_c} \right) - \frac{1}{2} \sqrt{\left(\frac{2 L_c}{S_c} - \sin^2 \theta \right)} \right\} \quad (72)$$

where, $r_c = \frac{V_{bdc}}{V_{tdc}}$

Differencing the above equation, the rate of change of volume of charge can be written as (32),

$$V^t(\theta) = \frac{dV}{d\theta} = \frac{V_{dts}}{2} \left\{ \frac{1}{2} \frac{\sin 2\theta}{\left[\left(\frac{r L_C}{S_r} \right)^2 - \sin^2 \theta \right]} - \sin \theta \right\} \quad (73)$$

3.2.3 Solution Procedure

Equations 25, 26, 27, 28, 29, 30, 31, 32, 33, 34, 35, 36, 37, 38, 39, 40, 41, 42, 43, 44, 45, 47, 48, 49, 50, 51, 52, 53, 54, 55, 57, 58, 64 and 73 formed the set of governing equations for pure gasoline operation as well as for methanol blended gasoline operation which are solved using Runge-Kutta fourth order scheme. Computerization started at EPO and closed at EPC.

4. RESULTS AND DISCUSSION

For any studies or investigations, mathematical simulation is necessary in order to predict the performance of the system. Then this simulation is to be validated with experimental methods and the results are to be correlated. In this investigation a zero-dimensional two-zone combustion model and a zero-dimensional multi-zone combustion model are assumed in order to predict the combustion characteristics which are shown in the subsequent paragraphs.

Fig-2 shows the variation of temperature of burned gases at EPO with crank angle with two-zone and multi-zone modeling for CE with gasoline, while Fig-3 shows the variation of temperature of burned gases at EPO with crank angle with two-zone and multi-zone modeling for CCE with methanol blended gasoline at peak load operation of the engine. Experimental values are also incorporated in these figures to note down the deviation between the experimental values and the values determined with mathematical modeling.

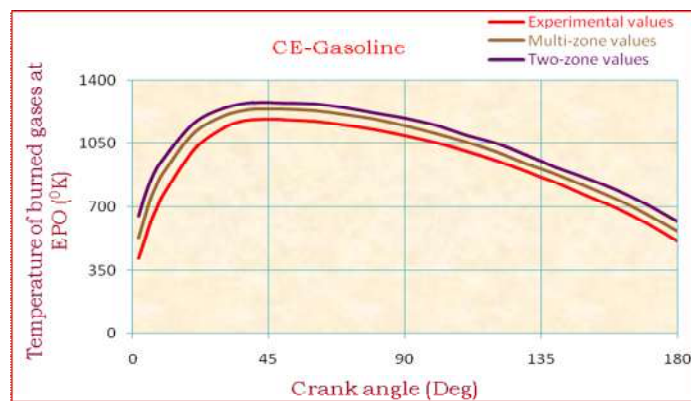


Figure 2 Variation of experimental results of temperature of burned gases ($^{\circ}\text{K}$) with crank angle (degrees) in CE with gasoline with the data of combustion zone models

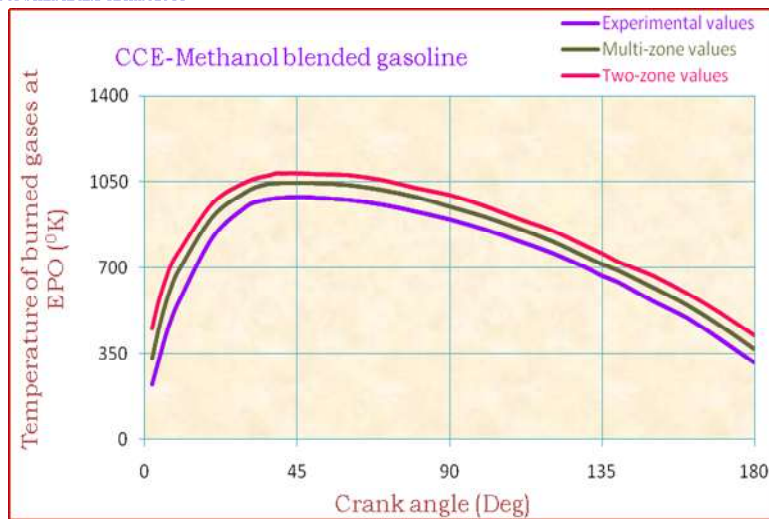


Figure 3 Variation of experimental results of temperature of burned gases ($^{\circ}\text{K}$) with crank angle (degrees) in CCE with methanol blended gasoline with the data of combustion zone models

The experimental value observed for CE with pure gasoline operation is 863°K , while with multi-zone modeling it was 910°K and with two-zone modeling it was 952°K . The deviation observed between the experimental results and theoretical values was due to the assumptions made in combustion models which may be far from the reality. However, a marginal deviation of 5 % is observed between the values obtained by experimentation and with multi-zone combustion modeling. The deviation between the two-zone combustion model and experimental values was observed to be 10 %, as the whole combustion phenomena is assumed to be burned zone and unburned zone while other zones are not taken in to consideration unlike in multi-zone combustion model. Similar trends are observed with the above figures. Hence, it was concluded that multi-zone combustion model gives the values nearer to the experimental data than two-zone combustion model.

Combustion characteristics obtained with different combustion models such as two-zone and multi-zone are to be validated with experimental results. Generally, temperature, pressure, PP, TOPP, MRPR, MHR and temperature of burned gases at EPO are the parameters where validation of the results is done. PP obtained with modeling is validated by experimental means obtained by P- θ software package and similarly other combustion parameters also. The temperatures are of two types-burned gas temperature and unburned gas temperature. The burned gas temperature at the exhaust port opening (EPO) is determined from the modeling and that is validated with the experimental means. The % deviation of the results obtained with the modeling and experimental results is then calculated.

Fig-4, Fig-5, Fig-6, Fig-7 and Fig-8 presents the bar charts which shows the variation of PP, MHR, TOPP, MRPR and temperature of burned gases at EPO in different versions of the engine with different test fuels at peak load operation of the engine by means of mathematical modeling and compared with experimental results.

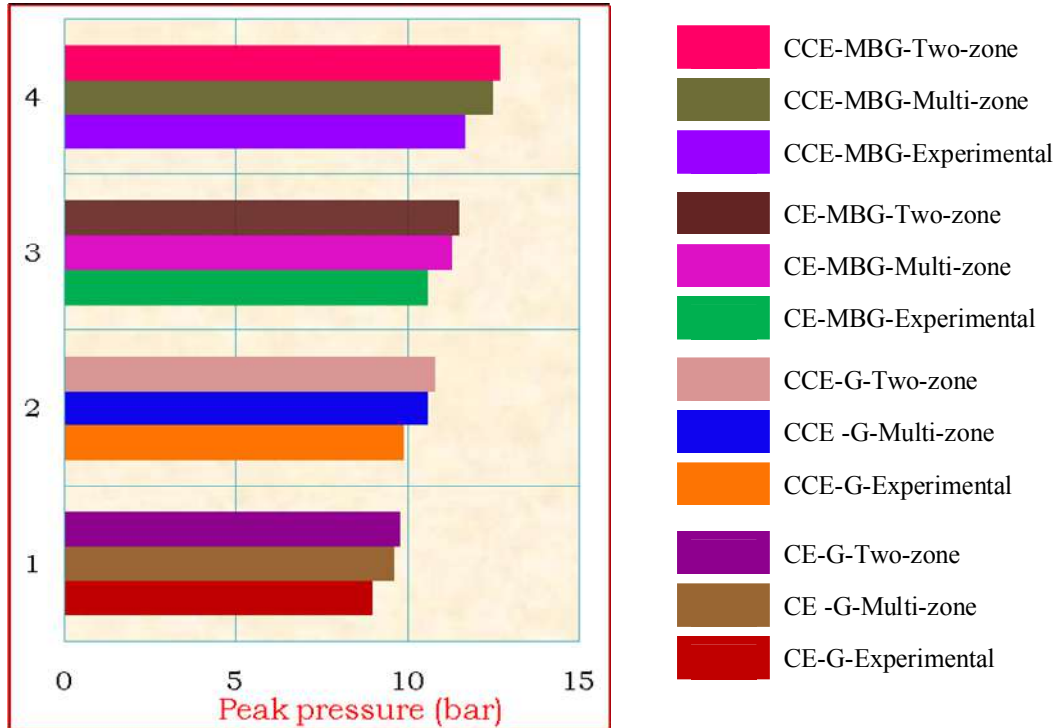


Figure 4 Bar chart showing the variation of peak pressure PP) (bar) in CE and CCE with test fuels

From the Fig-4, it is observed that copper coated engine (CCE) shows higher value of PP with different test fuels in comparison with pure gasoline operation in conventional engine (CE). As indicated with the experimental values as well as the values determined with combustion models, multi-zone model shows the value of PP nearer to the experimental value (the deviation being 7%) with different versions of the engine with different test fuels, while two-zone model predicted the values of PP at 9% higher than experimental values, which shows the assumptions made in two-zone model are far from reality.

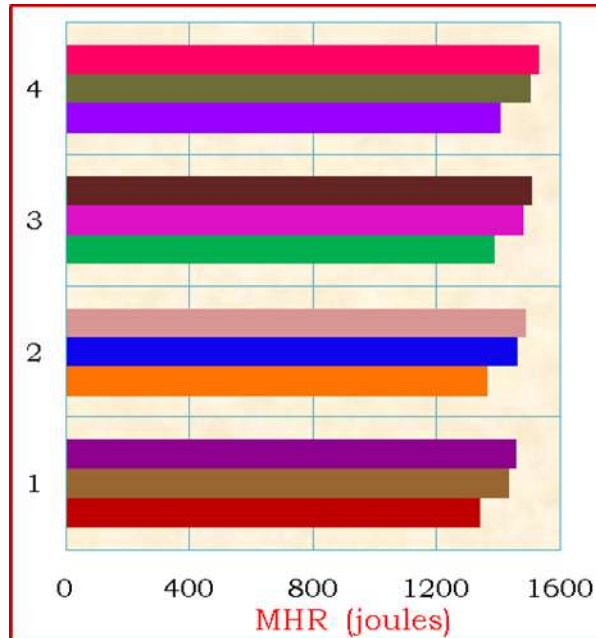


Figure 5 Bar chart showing the variation of MHR (joules) in CE and CCE test fuels

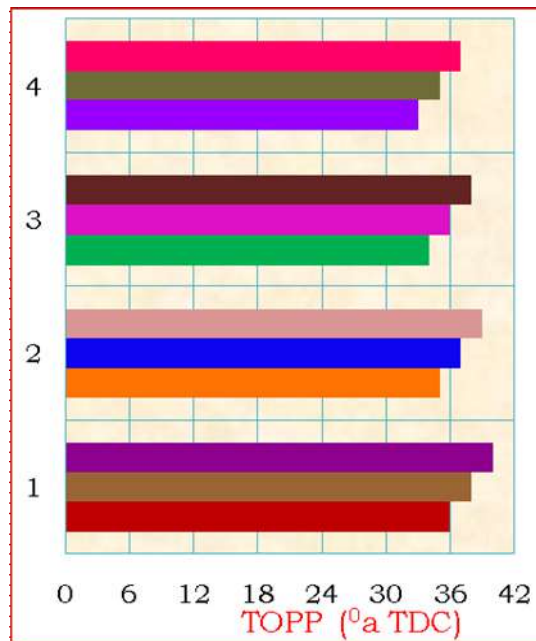


Figure 6 Bar chart showing the variation TOPP in CE and CCE with with test fuels

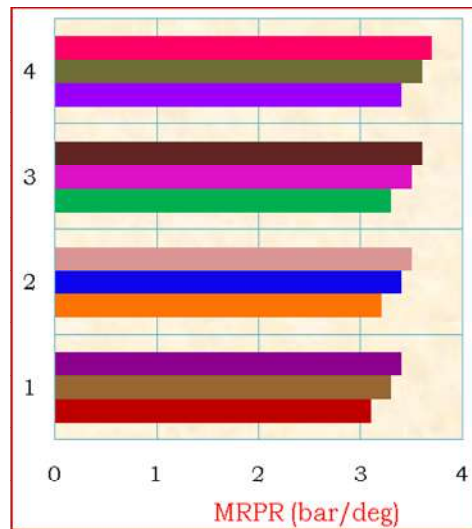


Figure 7 Bar chart showing the variation of MRPR (bar/deg) in CE and CCE with test fuels

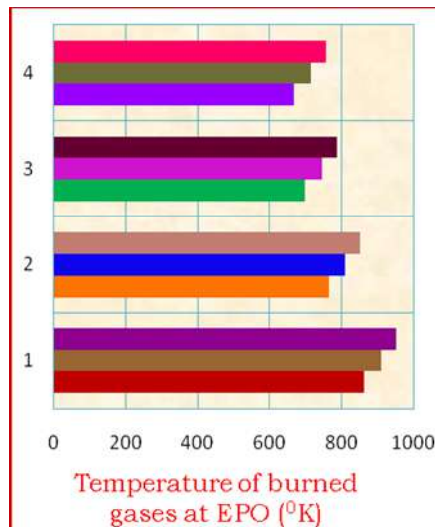


Figure 8 Bar chart showing the variation of temperature of burned gases at EPO (°K) in CE and CCE with test fuels

It is necessary to validate the theoretical results determined with mathematical modeling or simulation with experimental results. Generally it can be done either comparing with experimental results or comparing with the data of other researcher. The author tries to predict the results with modeling and compared with experimental results and validated with the data of other researcher also.

Fig-9 shows the variation of pressure with crank angle in CCE for methanol blended gasoline operation determined by the author by means of multi-zone combustion model. In the same graph the variation of pressure in CE with pure gasoline operation found out by experimental means is also shown



for comparison purpose. The trends of the graph are exceedingly coinciding well and hence it is established that the data predicted by the author is reasonably well.

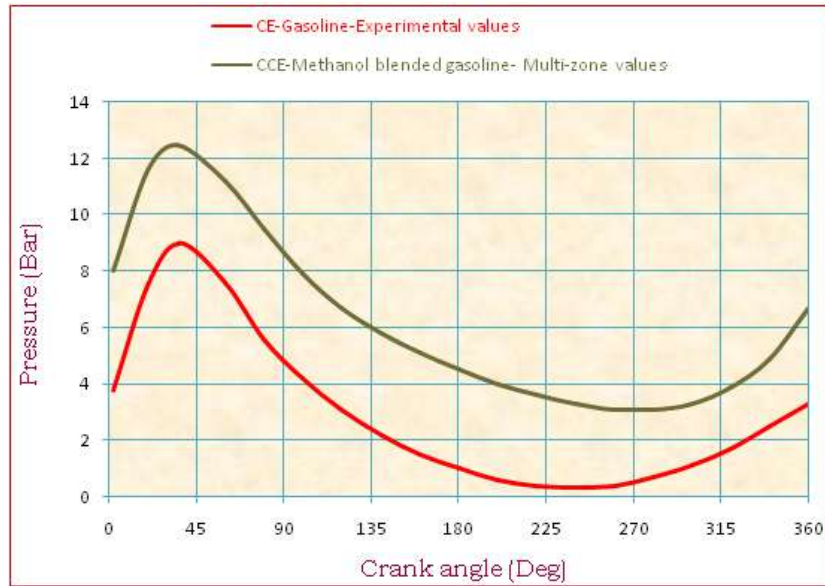


Figure 9 Variation of pressure with crank angle for validation of the results of the author

Fig-10 shows the variation of heat release with crank angle in CCE for methanol blended gasoline operation determined by the author by means of multi-zone combustion model. In the same graph the variation of heat release in CE with pure gasoline operation found out by experimental means is also shown for comparison purpose. The trends of the graph are exceedingly coinciding well and hence it is established that the data predicted by the author is reasonably well.

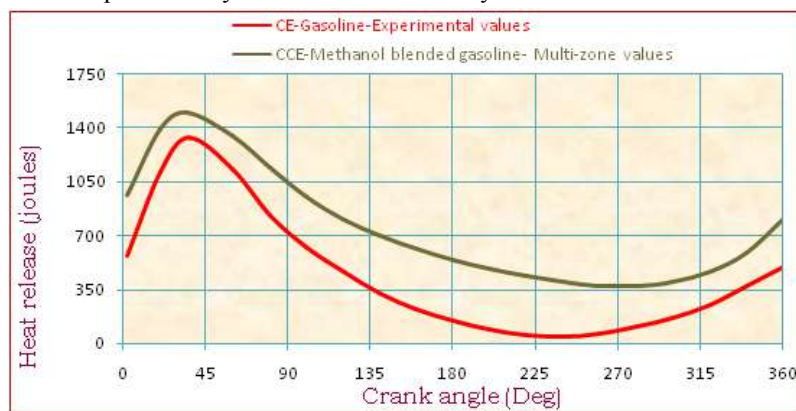


Figure 10 variation of heat release with crank angle for validation of the results of the author

Fig.11 shows the variation of temperature of burned gases at EPO with crank angle in CCE for methanol blended gasoline operation determined by the author by means of multi-zone combustion model. In the same graph the variation of heat release in CE with pure gasoline operation found out by



experimental means is also shown for comparison purpose. The trends of the graph are exceedingly coinciding well and hence it is established that the data predicted by the author is reasonably well.

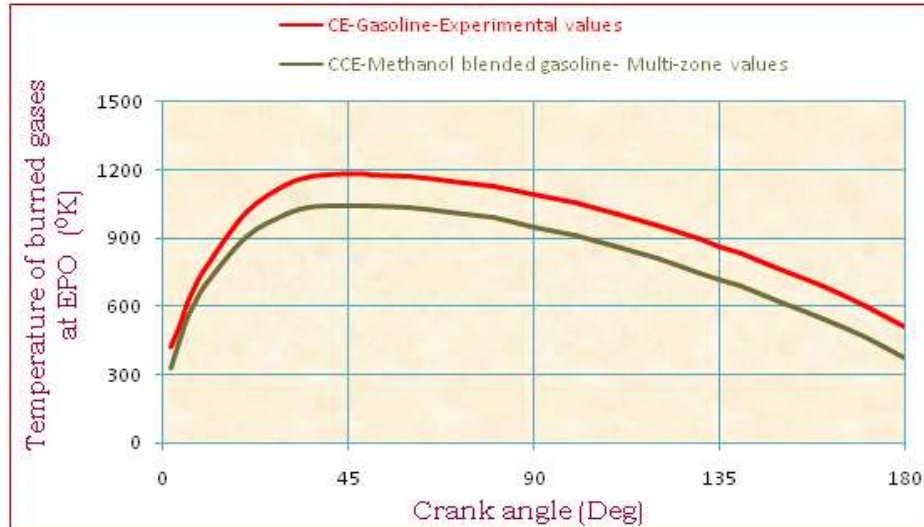


Figure 11 variation of temperature of burned gases at EPO with crank angle for validation of the results of the author

From the Fig-9, Fig-10 and Fig-11, it is concluded that the data of the author is coinciding well not only in magnitude but also trends are exceptionally well. It is concluded that the multi-zone combustion model gave values nearer to experimental values in determining PP. This is also depicted in the Fig-5 (variation of TOPP), Fig-6 (variation of MRPR), Fig-7 (variation of MHR) and Fig-8 (variation of temperature of burned gases at EPO). Hence it is concluded that the combustion characteristics predicted by multi-zone combustion model are very close to those of experimental values, which validate the data determined with experimentation.

5. CONCLUSIONS

1. PP increased by 30 % with methanol blended gasoline in CCE over pure gasoline operation on CE.
2. TOPP decreased by 8.3 % with methanol blended gasoline in CCE over pure gasoline operation on CE.
3. MRPR increased by 10 % with methanol blended gasoline in CCE over pure gasoline operation on CE.
4. MHR increased by 5 % with methanol blended gasoline in CCE over pure gasoline operation on CE.
5. Temperature of burned gases at EPO decreased by 22.6 % with methanol blended gasoline in CCE over pure gasoline operation on CE.
6. The deviation in the combustion characteristics like PP, TOPP, MRPR, MHR and temperature of burned gases at EPO obtained with multi- zone combustion model is found to be 7% over experimental values.

6. ACKNOWLEDGEMENTS

Authors thank authorities of Chaitanya Bharathi Institute of Technology, Hyderabad for providing facilities for carrying out research work. Financial assistance provided by All India Council for Technical Education (AICTE), New Delhi, is greatly acknowledged.

7. REFERENCES

1. Murali Krishna, M.V.S., Kishor, K., Murthy, P.V.K., Gupta, A.V.S.S.K.S. and Narasimha Kumar, S. Performance evaluation of copper coated spark ignition engine with gasohol with catalytic converter, *International Journal of Engineering Studies*, Volume-2; Number-4; 2010; 465-473.
2. Murali Krishna, M.V.S. and Kishor, K., Investigations on catalytic coated spark ignition engine with methanol blended gasoline with catalytic converter, *Indian Journal (CSIR) of Scientific and Industrial Research*, Volume-67; 2008; 543-548.
3. Murthy, P.V.K., Murali Krishna, M.V.S., Narasimha Kumar, S., Kishor, K. and Giridhar Reddy, P. Performance of copper coated two stroke spark ignition engine with alternate fuels with catalytic converter, *International Journal of Engineering & Techno-science*, Volume-2; Number-2; 2011; 145-149.
4. Benson, R.S., Annand, W.J.D. and Baruatt, P.C. A simulation model including intake and exhaust systems for a single cylinder four-stroke cycle spark ignition engine, *International Journal of Mechanical Sciences*, Volume-17; Number-2; 1975; 97-124.
5. Gatowski, J.A., Balles, E.N., Nelson, F.E., Ekchian, J.A. and Heywood, J.B. Heat release analysis of engine pressure data, *SAE paper*, Number-841359; 1985; 5,961-5,977.
6. Paulina, S. Kuo. Cylinder pressure in a spark-ignition engine: A computational model, *Journal of Undergraduate Sciences*, Volume-3; 1996; 141-145.
7. Ivan Arsie., Cesare Pianese. And Gianfranco Rizzo. Models for the prediction of performance and emissions in a spark ignition engine-a sequentially structured approach, *SAE paper No- 980779*, 1998.
8. Van Leersum, J. A numerical model of a high performance two-stroke engine, *Applied Numerical Mathematics*, Volume-27; Issue-1; 1998, 83-108.
9. Chan, S. H. and Zhu, J. Modeling of engine in-cylinder thermodynamics under high values of ignition retard, *International Journal of Thermal Sciences*, Volume-40; 1999; 94-103.
10. Nedunchezian, N. and Dhandapani, S. Heat release analysis of lean burn catalytic combustion in a two-stroke spark ignition engine, *Combustion Science and Technology*, Volume-155; Number-1; 2000181 – 2000.
11. Sitthiracha, S, Patumsawad, S. and Koetnuyom, S. An analytical model of spark ignition engine for performance prediction, *Proceedings of the 20th Conference of Mechanical Engineering Network*, Thailand, 2006.
12. Harish Kumar, R. and Antony, A.J. Progressive combustion in SI-engines—experimental investigation on influence of combustion related parameters, *Saadhana*, Volume-33; Part-6; 2008; 821–834.
13. Nirendra, N. and Mustafi Robert, R. Raine. Application of a spark ignition engine simulation tool for alternative fuels, *Journal of Engineering for Gas Turbines and Power*, Volume-130; 012804-1-6; 2008.



14. Hosseini, S., Abdolah, R. and Khani, A. A developed quasi-dimensional combustion model in spark ignition engines, Proceedings of the World Congress on Engineering, London, 2008.
15. Verhelst, S. and Sheppard, C.G.W. Multi-zone thermodynamic modeling of spark-ignition engine combustion – an overview, Energy Conversion and Management, Volume-50; Number (Issue)-5; 2009, 1326-1335.
16. Agarwal, A., Filipi, Z.S., Assanis, D.N. and Baker, D.M. Assessment of single- and two-zone turbulence formulations for quasi-dimensional modeling of spark-ignition engine combustion, Combustion Science and Technology, Volume-136; 1998, 13-39.
17. Vancoillie, J. and Verhelst, S. Modeling the combustion of light alcohols in SI engines: a preliminary study, In FISITA 2010 World Automotive Congress, Budapest, Hungary, 2010.
18. Aleonte, Mihai, Cosgarea, Radu, Cofaru, Corneliu, Beck, Kai, velji, Amin spicher. and Ulrich. Combustion and emissions analysis of different alcohol blends in a two – stroke SI engine, International automotive congress- Conat 2010
19. Farag A.El Fatih., El-Mallah A.Abd El Kader. Ali S. Mohammed. and Gad M. saber., “Investigations on the combustion modeling of gaseous fuels, European Journal of Scientific Research, Volume-46; Number-4; 2010, 563-573.
20. Jiri Hvezda. Multi-zone models of combustion and heat transfer processes in SI Engines, SAE Technical Paper, 2011- 37-0024, 2011.
21. Lounici, Mohand Said. Loubar, Khaled., Balistrout, Mourad. and Tazerout, Mohand., Investigation on heat transfer evaluation for a more efficient two-zone combustion model in the case of natural gas SI engines, Applied Thermal Engineering, Volume 31; Issue 2; 2011; 319-328.
22. Heywood, J.B. Internal Combustion Engine Fundamentals, Thermo-chemistry of fuel air mixtures, Properties of working fluids, McGraw-Hill Book Company, New York, 85-96 and 130 –140; 1988.
23. Heywood, J.B., Higgins, J.M., Watts, P.A. and Tabaczynski, R.J. Development and use of a cycle simulation to predict SI engine efficiency and NO_x emissions, SAE Paper No-790291, 1979.
24. Woschni, G. A universally applicable equation for the instantaneous heat transfer co-efficient in the internal combustion engine, SAE paper No-670931, 1967.
25. Ferguson, Colin R. and Allan Thomson Kirkpatrick., Internal combustion engines: applied thermo sciences, John Wiley & sons; 2001.
26. Lavoie, G.A., Heywood, J. B. and Keck, J. C. Experimental and theoretical investigation of nitric oxide formation in internal combustion engines, Combustion Science and Technology, Volume-1; 1970, 313-326.
27. Press, W.H., Flannery, B.P., Teukolsky, S.A. and Wetterling, W.T. Numerical recipes: the art of scientific computing, Cambridge University Press, 1986.
28. Ramos, J.I. Internal combustion engine modeling”, Hemisphere Publishing Corporation, New York, 1989.
29. Annand, W.J.D., Heat transfer in the cylinder of reciprocating internal combustion engines, Proceedings of Institution of mechanical engineers, Volume 177; Number 36; 1963.
30. Murali Krishna, M.V.S., Performance evaluation of low heat rejection (LHR) diesel engine with alternative fuels, Ph. D. Thesis, JNT University, Hyderabad, 2004.

- 31.Jagadeesan, T.R. and Mathu, S. Analytical and experimental investigations of ethanol diesel dual fuel combustion system, Proceedings of .VI International Symposium on Alcohol Fuel Technology, Canada, 1984; 194-201.
- 32.Ganesan, V. Computer simulation of spark ignition engine processes, University Press (India) Limited, Hyderabad, 1996.
- 33.JANAF Thermo chemical Tables, 2nd Edition, NSRDS-NB537, U.S National Bureau of Standards, June, 1971.
- 34.Rossine, F.D., Pitzer, K.S., Arnett, R.L., Braun, R.M. and Primentel. G.C. Selected values of physical and thermodynamic properties of hydrocarbons and related compounds, Carnegie Press, Pittsburgh, 1953.

K. Kishor¹, A.V.S.S.K.S.Gupta², M.V.S.Muralikrishna¹, S. Narasimha Kumar¹ and P.V. Krishna Murthy^{3*}

¹Mechanical Engineering Department, Chaitanya Bharathi Institute of Technology, Gandipet, Hyderabad- 500 075

² Mechanical Engineering Department, J.N.T. University, Hyderabad- 500 085

³Vivekananda Institute of Science and Information Technology, Shadnagar, Mahabubnagar-509216, *E-mail: Krishnamurthy_venkata@yahoo.co.in